

Geometry-Specific Scaling of Detonation Parameters from Front Curvature

Scott I. Jackson and Mark Short
Shock and Detonation Physics Group, Los Alamos National Laboratory,
Los Alamos, NM 87544

1 Introduction

It has previously been asserted that classical detonation curvature theory predicts that the critical diameter and the diameter-effect curve of a cylindrical high-explosive (HE) charge should scale with twice the thickness of an analogous two-dimensional HE slab [1–3]. The varied agreement of experimental results [1–4] with this expectation have led some [1–3] to question the ability of curvature-based concepts to predict detonation propagation in non-ideal HEs. This study addresses such claims by showing that the expected scaling relationship (hereafter referred to $d = 2t$) is only consistent with curvature-based Detonation Shock Dynamics (DSD) theory [5] under special limiting circumstances.

Detonation Velocity and Wavefront Curvature: It has long been known that the detonation phase velocity D_0 of a condensed-phase explosive will decrease with increasing flow divergence in the detonation reaction zone (RZ) [6]. This divergence occurs when post-shock pressures exceed the yield stress of the HE's confiner and results in the transverse expansion of flow behind the shock front (Fig. 1). The onset of transverse flow ahead of the sonic locus induces curvature of the shock front. As the charge diameter d decreases, so does the ratio of the energy driving the shock relative to the energy lost to flow expansion, resulting in a decreased D_0 . In cylindrical charges, this velocity decrement with diameter is referred to as an HE's diameter effect. Figure 2 shows an example of this behavior from Ref.[7] for neat nitromethane (NM) and a NM-silica-guar mixture. The decreased detonation velocities and flow divergence can decrease the post-shock temperatures and delay more of the chemical energy release to behind the sonic locus of the RZ. The detonation will fail below a critical limit where detonation shock and RZ coupling can no longer be maintained. In practice, the charge diameter corresponding to this limit is defined as the failure diameter d_c . Such losses can also be present in gas-phase detonation [8], although in controlled experiments the lower pressures achieved in gas-phase detonation rarely exceed the yield stress of most metal confiners. However, flow divergence can still result from frictional and thermal losses in the RZ flow [9].

2 The Curvature-Based Theory of Detonation Shock Dynamics

Detonation Shock Dynamics (DSD) is a surface propagation concept that replaces the detonation shock and RZ with a surface that evolves according to a specified normal velocity evolution law. There are three classes of propagation that are nominally encompassed within DSD.

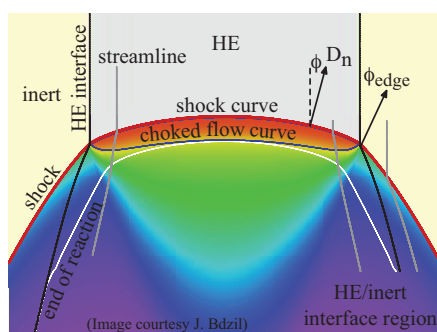


Fig. 1: Flow divergence and curvature.

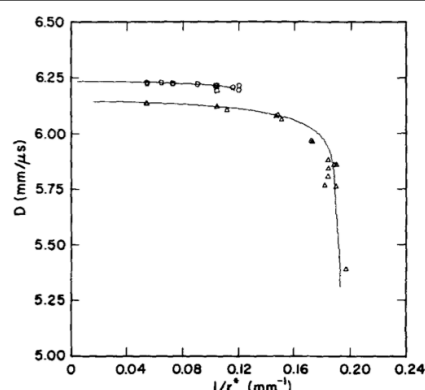


Fig. 2: Diameter effect for NM mixtures [7].

Huygens construction: For a detonation with no RZ thickness (a limiting asymptotic theory), the detonation collapses to a surface. The normal detonation surface velocity D_n at each point is D_{CJ} (a constant). In this case the surface evolves as a standard Huygens wave front reconstruction. Since all detonations have some finite thickness, the Huygens construction is an idealized case. However, conventional HEs (sometimes called ideal) like HMX-based PBX 9501 have a sufficiently short RZ (a few 100s of microns) that a Huygens approximation of the front propagation is reasonable.

DSD D_n - κ theory: Detonation shock dynamics accounts for the effect of the finite thickness of the detonation reaction wave on D_n . It has a rational asymptotic basis, developed by Bdzil [10] and Bdzil & Stewart [5, 11], assuming weak curvature and slowly evolving limits. Specifically, it assumes that the detonation curvature is small relative to the inverse of the length of the detonation zone, and that the wave evolve slowly relative to particle passage through the RZ. To leading order, D_n is constant, with the first correction being a function of shock curvature. The specific velocity versus curvature relation is determined by a balance between heat release, the energy lost to flow divergence due to curvature of the front, and the amount of heat release cut-off due to the location of the sonic locus within the RZ. In this way, the detonation shock and RZ can be replaced with a single surface whose normal velocity is prescribed as a function of curvature. This is the basis behind the fitting of detonation front shapes for a range of HEs to a “ D_n - κ law,” written as

$$\kappa = f(D_n) \text{ or } D_n = f(\kappa) \quad (1)$$

Importantly, note that κ is geometry independent, representing the sum of the principal curvatures for any three-dimensional surface. In a slab geometry, there is only one component of curvature. In an axisymmetric rate-stick geometry, the total curvature is the sum of the slab geometry curvature plus an axisymmetric component, and these two components are not generally equal (except on the charge axis). Ideal HEs like PBX 9501 and nitromethane, as well as many insensitive HEs like TATB-based PBX 9502 are expected to have a reasonable correspondence to a D_n - κ behavior. For instance, the shapes obtained from PBX 9502 rate sticks have reasonable overlap [12].

Higher-order Detonation Shock Dynamics: For non-ideal HEs, the increased size of the detonation RZ (e.g. up to several cms for ANFO), means that the basic D_n - κ law is not sufficient to represent the dynamics driving the wavefront. Time-dependent and transverse flow contributions become increasingly important in determining the wave shape. With non-negligible transverse flow terms, the propagation dynamics are no longer geometry independent. For instance, in ANFO rate sticks, the D_n - κ curves for different size sticks no longer overlap [13]. Note that even near the edge of steady IHE (like PBX 9502) rate-stick charges, the rapid increase in curvature likely means that significant transverse arc length flow variations influence the wave shape and thus D_n - κ fits near the edge are not likely to overlap for different charge sizes. Higher-order theories have been developed [14] to address this case.

3 The Specifics of DSD Theory

Assume an axisymmetric detonation propagating in the positive z direction in a cylindrical system. The DSD surface is given by $z = z_s(r)$, with a surface normal orientated upwards. The DSD propagation law in which the curvature is a function of normal detonation velocity can be represented by

$$\kappa = f(D_n). \quad (2)$$

Note the curvature here is the total surface curvature, and the above is independent of geometry. Thus for a given HE, $f(D_n)$ is fixed for the same initial state of a given HE. Defining the level set function as $S = z_s(r) - z$, the normal to the surface is

$$\mathbf{n} = -\frac{\nabla S}{|\nabla S|} = \frac{1}{\sqrt{1 + [d(z_s(r))/dr]^2}} \left(-\frac{d}{dr} z_s(r) \mathbf{e}_r + \mathbf{e}_z \right). \quad (3)$$

The curvature for the cylindrical geometry is then

$$\kappa_c = \nabla \cdot \mathbf{n} = -\frac{z_s''(r)}{\left(1 + [z_s'(r)]^2\right)^{3/2}} - \frac{z_s'(r)}{r \left(1 + [z_s'(r)]^2\right)^{1/2}}. \quad (4)$$

The second term of the above equation is the axisymmetric contribution κ_a and would not be present in a planar slab geometry, where

$$\kappa_s = -\frac{z_s''(r)}{\left(1 + [z_s'(r)]^2\right)^{3/2}}. \quad (5)$$

With D_n as the normal component of the detonation velocity and D_0 as the steady axial component, we define ϕ as the angle between the axial direction and the surface normal \mathbf{n} ,

$$\cos \phi = \frac{D_n}{D_0} = \frac{1}{|\nabla S|} = \frac{1}{\left(1 + [z_s'(r)]^2\right)^{1/2}}, \quad \frac{dz_s}{dr} = -\tan \phi. \quad (6)$$

The total curvature in the cylindrical geometry is then given by

$$\kappa_c = \kappa_s + \kappa_a = \kappa_s + \frac{\sin \phi}{r} \quad (7)$$

Geometric considerations can be used to rewrite the above theory in terms of wavefront path length ξ and ϕ

$$\frac{dr}{d\xi} = \cos \phi, \quad \frac{dz}{d\xi} = -\sin \phi, \quad \kappa_s = \frac{d\phi}{d\xi}, \quad (8)$$

yielding

$$\frac{dr}{d\phi} = \frac{\cos \phi}{\kappa_s}, \quad \frac{dz}{d\phi} = -\frac{\sin \phi}{\kappa_s} \quad (9)$$

Equations 2, 6, 7, and 9 can be solved subject to $z(0) = 0$, $r(0) = 0$, and a specified charge edge angle that is specific to each HE/inert interaction, $\phi = \phi_{edge}$. This requires either D_0 be known, in which case r_{edge} is determined by a single integration, or r_{edge} be given in which case D_0 would be determined by a sequence of iterations.

4 Slab vs. Cylindrical Curvature Theory

Previous authors [1–3] have implicitly and imprecisely assumed that a detonation front in a cylindrical charge is quasi-spherical, with identical curvature in two orthogonal dimensions. With the additional assumption that a slab geometry only has curvature in a single direction, it can be reasoned that both geometries would yield identical D_0 when the slab thickness is equivalent to one half the diameter of the cylindrical charge, $d = 2t$. The critical thickness and diameter are expected to follow a similar relationship $d_c = 2t_c$ [1, 2], implying shock and RZ coupling is dependent on a critical D_0 or curvature value. (Sketches of the relevant geometries are in Fig. 1 of Ref. 1.) Experiments with non-ideal HEs have shown variations in this proposed scaling, from the expected value of two [2] to values as large as four [1, 3]. Such deviations have been cited as indications that global detonation propagation in non-ideal HEs is not solely dependent on curvature concepts [3].

However, curvature theory demonstrates that the $d = 2t$ scaling will only occur when: (i) the detonation be sufficiently ideal that a $\kappa = f(D_n)$ relation be valid; (ii) the two components of cylindrical curvature, κ_s and $\kappa_a = \sin \phi / r$, be identical. For a slab, $\kappa_s = f(D_n)$, implying

$$\frac{dr_s}{d\phi} = \frac{\cos \phi}{f(D_n)}, \quad \frac{dz_s}{d\phi} = -\frac{\sin \phi}{f(D_n)}, \quad z_s(0) = 0, \quad r_s(0) = 0, \quad \phi = \phi_{edge}. \quad (10)$$

Putting $(\sin \phi) / r = \kappa_s$, in a cylinder $2\kappa_s = f(D_n)$, and

$$\frac{d(r_c/2)}{d\phi} = \frac{\cos \phi}{f(D_n)}, \quad \frac{d(z_c/2)}{d\phi} = -\frac{\sin \phi}{f(D_n)}, \quad z_{rs}(0) = 0, \quad r_c(0) = 0, \quad \phi = \phi_{edge}. \quad (11)$$

In order to get the same D_0 between a slab and a cylindrical rate-stick,

$$r_c = 2r_s, \quad z_c = 2z_s, \quad (12)$$

i.e. the $d = 2t$ scaling discussed. In practice, the curvature component κ_s will not be equivalent to the axisymmetric curvature component $(\sin \phi) / r$. Consequently to obtain an equivalent D_0 , $r_{rs} \neq 2r_s$. The only wave profile that would satisfy Eq. 12 would be circular such that $z_s(r) = \sqrt{a^2 - r^2}$. Such a geometry would result in a spherical detonation front for the cylindrical rate stick and a cylindrical detonation front for the slab. More generally, if one assumes κ_a and κ_s are related (idealistically) through the relation $\kappa_a = \alpha \kappa_s$, an equivalent D_0 is found when $1/d = (1/2t)[2/(1 + \alpha)]$. Thus for $\alpha < 1$, the scaled diameter effect curve for the slab (D_0 vs. $1/2t$) lies to the left of that for the rate-stick (D_0 vs. $1/d$). When $\alpha > 1$, i.e. $\kappa_a > \kappa_s$ the converse is true. The situation for $\alpha > 1$ has been observed experimentally [1–3] for non-ideal HE.

Fig. 3 contains the curvature components for a PBX 9502 cylindrical rate stick with radius $R = 9$ mm [12]. The black line is the total curvature $\kappa_s + \kappa_a$, the blue line is the axisymmetric curvature κ_a , and the green line is κ_s for the cylinder. The purple line is $(\kappa_a - \kappa_s) / \kappa_a$, which represents the difference between the two components. The wave profile is perfectly spherical when $(\kappa_a - \kappa_s) / \kappa_a = 0$. In this range, the wave can be well-represented as a Huygens construction and the $d = 2t$ scaling would apply. However, deviations from $(\kappa_a - \kappa_s) / \kappa_a = 0$ indicate an increasingly non-spherical wave shape. In this regime, detonation propagation will vary from the $d = 2t$ scaling as described above, necessitating the use of DSD theory. In practice, detonation in *ideal* HEs may not deviate significantly from this shape, resulting in a scaling close-to (but not exactly) $d = 2t$. *Non-ideal* HEs cannot approximate this scaling due to the increased dependence on time and transverse flow. Thus, it is not reasonable to expect $d = 2t$ scaling, or even a constant scaling value, to apply to non-ideals.

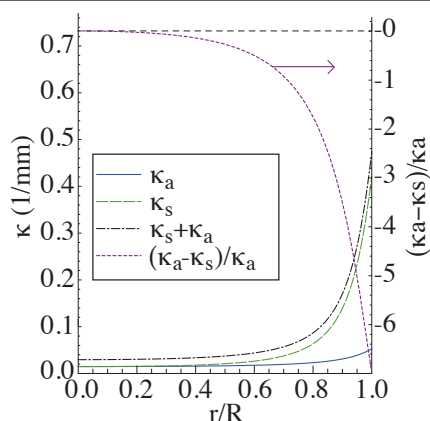


Fig. 3: Cylindrical curvature components.

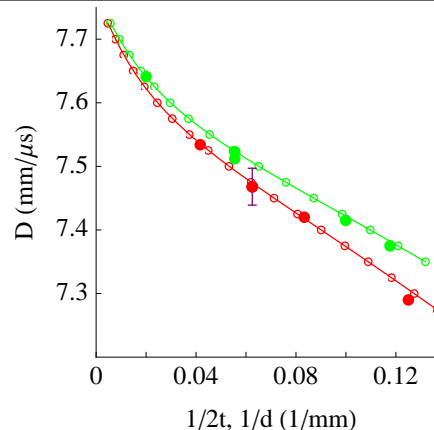


Fig. 4: PBX 9502 size-effect data.

5 Calculation and Experimental Verification of the Scaling Relationship

The $D_n(\kappa)$ form of DSD theory predicts that the scaling of the diameter- and thickness-effect curves will be a function of the form of the $D_n(\kappa)$ relation, allowing computation of curves for HEs that are calibrated to the DSD model. Calibration requires testing in only one geometry (Eq. 2), traditionally the cylindrical rate-stick. The computed PBX-9502 thickness-effect curve based on a PBX-9502 Lot-008 rate-stick DSD calibration by Bdzil (private communication) is shown in red and the diameter-effect curve is shown in green in Fig. 4. Open symbols correspond to each calculation point. For PBX 9502, the computations show that the $d = 2t$ scaling approximately holds for large charges where the detonation is flatter, but as differences between κ_s and κ_a become significant for smaller diameter charges, the size-effect (composing both diameter- and thickness-effect) curves deviate from the $d = 2t$ scaling, with the scaled cylinder curve increasing above the slab curve. D_n - κ theory predicts such behavior: The larger magnitude of κ_s than κ_a along the front shown in Fig. 3 is consistent with the DSD size-effect curves calculated in Fig. 4.

Matched experimental front-curvature and size-effect data in both the cylindrical and slab geometries from identical HEs is sparse in the literature. However, limited quantities are available for Lot-008 PBX 9502. The solid symbols in Fig. 4 represent the available unconfined cylindrical data (green) [12] compared to five (red) unconfined slab tests (fielded for this study) and a single (purple) PMMA-confined slab data point [15]. (PMMA confinement of PBX 9502 is equivalent to no confinement as far as D_0 and curvature parameters are concerned.) Error bars for all experimental data points are encompassed by the symbols, except for the PMMA-confined test. Overall, experiment and calculation for both geometries agree very well, illustrating that curvature-based theory is capable of properly predicting the scaling of the size-effect curves and that this scaling relationship is not necessarily $d = 2t$.

We will present additional velocity and curvature measurements in the slab geometry for DSD-calibrated HEs. Experimental slab-geometry data will then be compared with computed thickness-effect curves to test the applicability of curvature-based D_n - κ theory to different classes of HEs, such as HMX-based PBX 9501 (ideal), PBX 9502 (non-ideal), and ANFO (highly non-ideal). Such an approach will yield the scaling relationship for each HE and the predictive ability of the D_n - κ implementation.

References

- [1] O. Petel, D. Mack, A. Higgins, R. Turcotte, and S. Chan, "Minimum propagation diameter and thickness of high explosives," *Journal of Loss Prevention in the Process Industries*, vol. 20,

- pp. 578–583, 2007.
- [2] V. V. Silvestrov, A. V. Plastinin, S. M. Karakhanov, and V. V. Zykov, “Critical diameter and critical thickness of an emulsion explosive,” Combustion, Explosion, and Shock Waves, vol. 44, no. 3, pp. 354–359, 2008.
- [3] A. Higgins, “Measurement of detonation velocity for a nonideal heterogenous explosive in axisymmetric and two-dimensional geometries,” in Shock Compression of Condensed Matter, pp. 193–196, American Institute of Physics, 2009.
- [4] J. Gois, J. Campos, and R. Mendes, “Extinction and initiation of detonation of NM-PMMA-GMB mixtures,” in Shock Compression of Condensed Matter, pp. 827–830, American Institute of Physics, 1996.
- [5] J. Bdzil and D. Stewart, “The dynamics of detonation in explosive systems,” Ann. Rev. Fluid Mech., vol. 39, pp. 263–292, 2007.
- [6] H. Jones, “A theory of the dependence of the rate of detonation of solid explosives on the diameter of the charge,” Provc. Royal Soc., Series A, vol. 1018, pp. 415–426, 1947.
- [7] R. Engelke and J. Bdzil, “A study of the steady-state reaction-zone structure of a homogenous and a heterogenous explosive,” Physics of Fluids, vol. 26, pp. 1210–1221, 1983.
- [8] E. Dabora, J. Nicholls, and R. Morrison, “Influence of a compressible boundary on propagation of gaseous detonations,” in Proceedings of the 10th International Symposium on Combustion, vol. 10, (Pittsburgh, PA), pp. 817–830, Combustion Institute, 1965.
- [9] J. Fay, “Two-dimensional gaseous detonations: Velocity deficit,” Physics of Fluids, vol. 2, pp. 283–289, 1959.
- [10] J. Bdzil, “Steady-state two-dimensional detonation,” Journal of Fluid Mechanics, vol. 108, pp. 195–226, 1981.
- [11] J. B. Bdzil, W. Fickett, and D. S. Stewart, “Detonation shock dynamics: A new approach to modeling multi-dimensional detonation waves,” in Ninth Symposium (Int.) on Detonation, pp. 730–742, Office of Naval Research, 1989.
- [12] L. Hill, J. Bdzil, W. Davis, and R. Critchfield, “PBX 9502 front curvature rate stick data: Repeatability and the effects of temperature and material variation,” in Ninth Symposium (Int.) on Detonation, pp. 331–341, Office of Naval Research, 2006.
- [13] M. Short, T. Salyer, T. Aslam, C. Kiyanda, J. Morris, and T. Zimmerley, “Detonation shock dynamics calibration for non-ideal HE: ANFO,” in Shock Compression of Condensed Matter, pp. 189–192, American Institute of Physics, 2009.
- [14] J. Bdzil, T. Aslam, and M. Short, “DSD front models: Nonideal explosive detonation in ANFO,” in Twelfth Symposium (Int.) on Detonation, pp. 409–417, 2002.
- [15] T. Aslam, S. Jackson, and J. Morris, “Proton radiography of PBX 9502 detonation shock dynamics confinement sandwich test,” in Shock Compression of Condensed Matter, vol. 1195, (Melville, NY), pp. 241–244, American Institute of Physics, 2009.